

Nanoscale

Accepted Manuscript



This is an *Accepted Manuscript*, which has been through the Royal Society of Chemistry peer review process and has been accepted for publication.

Accepted Manuscripts are published online shortly after acceptance, before technical editing, formatting and proof reading. Using this free service, authors can make their results available to the community, in citable form, before we publish the edited article. We will replace this *Accepted Manuscript* with the edited and formatted *Advance Article* as soon as it is available.

You can find more information about *Accepted Manuscripts* in the [Information for Authors](#).

Please note that technical editing may introduce minor changes to the text and/or graphics, which may alter content. The journal's standard [Terms & Conditions](#) and the [Ethical guidelines](#) still apply. In no event shall the Royal Society of Chemistry be held responsible for any errors or omissions in this *Accepted Manuscript* or any consequences arising from the use of any information it contains.



Synthesis and Assembly of Barium-doped Iron Oxide Nanoparticles and Nanomagnets

Received 00th August 2015,
Accepted 00th ##### 2015

Liheng Wu, Bo Shen and Shouheng Sun*

DOI: 10.1039/x0xx00000x

www.rsc.org/

A facile organic-phase synthesis of monodisperse barium-doped iron oxide (Ba-Fe-O) nanoparticles (NPs) is reported. The Ba-Fe-O NPs can be converted into hexagonal barium ferrite NPs at 700 °C, showing strong ferromagnetic properties with H_c reaching 5260 Oe and M_s at 54 emu/g. Moreover, the Ba-Fe-O NPs can be assembled into densely packed magnetic arrays, providing a unique model system for studying nanomagnetism and for nanomagnetic applications.

Magnetic iron oxide nanoparticles (NPs) with controlled size and magnetic properties have attracted tremendous research and development interests due to their great application potentials for future nanomedicine,^{1–8} high performance ferrite magnets,^{9–11} and high density magnetic tape recording.^{11–13} There are two common types of magnetic iron oxides: the cubic structured spinel-type ferrites with a general formula MFe_2O_4 ($M = Mn, Fe, Co, Ni, \text{etc}$) and hexagonal barium ferrite, or BaFe, with a general formula $BaFe_{12}O_{19}$. The spinel ferrites are magnetically isotropic and weakly ferrimagnetic. In contrast, the hexagonal BaFe support anisotropic spin alignment along the crystallographic c -direction and their magnetocrystalline anisotropy can reach $5 \times 10^5 \text{ J/m}^3$.^{14,15} This, plus their chemical stability, makes BaFe a class of well-known permanent magnet materials.¹¹ Recently, the hard magnetic BaFe were also prepared in nanostructured plates and tested as a new medium for magnetic tape recording.^{16–20} To maximize the magnetic recording density in tape recording media and magnetic energy storage capability in ferrite magnets, uniform BaFe NPs with controlled magnetic properties need to be prepared and assembled in either two dimensional (2D) arrays (for magnetic recording) or densely-packed 3D stacks (for permanent magnets).

BaFe is normally synthesized by solid-state reactions between Ba- and Fe-precursors at temperatures higher than 1000 °C due to the need to form hexagonal structure from the

normal cubic oxide precursors.^{21–23} These include the direct solid reaction between metal hydroxides^{24,25} or iron oxide and barium carbonate,^{26–28} hydrothermal reaction of metal hydroxides followed by annealing,^{29–31} and organic phase preparation of $Fe_3O_4/BaCO_3$ core/shell NPs followed by annealing in O_2 .³² However, these solid state reactions and high temperature annealing often result in incomplete alloy formation between the Ba- and Fe-oxides. The high temperature diffusion between Ba- and Fe-precursors also causes uncontrolled sintering of BaFe, making it extremely difficult to control BaFe sizes and magnetic properties. To develop a better approach to BaFe NPs and their assemblies, we tested the organic-phase decomposition of both Fe- and Ba-precursors at temperatures above 200 °C. We found that Ba-doped iron oxide NPs, denoted as Ba-Fe-O NPs, could be easily prepared by thermal decomposition of $Fe(acac)_3$ ($acac = \text{acetylacetonate}$) and $Ba(\text{stearate})_2$ at 320 °C in 1-octadecene with oleic acid and oleylamine as surfactants. The as-synthesized Ba-Fe-O NPs were well-dispersed in hexane and could be easily assembled into 2D arrays. Upon thermal annealing, these NPs were converted to hexagonal BaFe NPs, showing much enhanced magnetic properties. Moreover, the synthesis could be generalized to make other doped iron oxide NPs, as demonstrated in the synthesis of strontium-doped iron oxide (Sr-Fe-O) NPs and hexagonal SrFe NPs. Here we highlight this new synthesis and self-assembly of Ba-Fe-O NPs to hexagonal BaFe magnet arrays.

To prepare Ba-Fe-O NPs, $Fe(acac)_3$ and $Ba(\text{stearate})_2$ were dissolved in 1-octadecene solution of oleic acid and oleylamine and the solution was heated at 320 °C for 1.5 h (See the ESI† for experimental details). Ba composition in the NP structure was analyzed by inductively coupled plasma–atomic emission spectroscopy (ICP–AES). In the synthetic condition with the amount of $Fe(acac)_3$ (300 mg) and oleic acid (1 mL) fixed, the composition of Ba in Ba-Fe-O NPs was controlled by the amount/concentration of $Ba(\text{stearate})_2$ or oleylamine (Table 1). For example, adding 20 mg of $Ba(\text{stearate})_2$ to the reaction mixture produced Ba-Fe-O NPs with a Ba/Fe atomic ratio of 0.04, denoted as $Ba_{0.04}\text{-Fe-O}$. 40 mg (or 60 mg) of $Ba(\text{stearate})_2$

Department of Chemistry, Brown University, Providence, Rhode Island 02912, USA.
Email: ssun@brown.edu; Fax: +1-401-863-9046; Tel: +1-401-863-3329

† Electronic Supplementary Information (ESI) available: Experimental details, Figure S1–S8. See DOI: 10.1039/x0xx00000x

gave $\text{Ba}_{0.055}\text{-Fe-O}$ (or $\text{Ba}_{0.065}\text{-Fe-O}$) NPs. In the synthesis, we also noticed that oleylamine played two roles in NP stabilization and in promoting metal precursor decomposition.^{33,34} Reacting 300 mg of $\text{Fe}(\text{acac})_3$ with 60 mg of Ba-stearate in 8 mL oleylamine and 7 mL 1-octadecene yielded $\text{Ba}_{0.075}\text{-Fe-O}$ NPs. By reducing the volume of 1-octadecene to 3 mL, $\text{Ba}_{0.082}\text{-Fe-O}$ NPs were obtained. These NPs have the Ba composition close to the ideal Ba/Fe ratio of 0.083 in the pure BaFe phase. If only oleylamine was used as the solvent, then $\text{Ba}_{0.095}\text{-Fe-O}$ NPs were synthesized. The Ba/Fe ratio of 0.095 is very close to the initial precursor ratio of $\text{Ba}(\text{stearate})_2/\text{Fe}(\text{acac})_3$ (0.099) used in the reaction, indicating almost complete precursor decomposition and metal ratio carry-over to the final Ba-Fe-O product.

Table 1. Experimental conditions for synthesizing Ba-Fe-O NPs with different Ba compositions (the amount of $\text{Fe}(\text{acac})_3$ and oleic acid was fixed to be 300 mg and 1 mL, respectively).

Reaction	$\text{Ba}(\text{stearate})_2$	Oleylamine	Octadecene	X in $\text{Ba}_x\text{-Fe-O}$
1	20 mg	6 mL	12 mL	0.040
2	40 mg	6 mL	12 mL	0.055
3	60 mg	6 mL	12 mL	0.065
4	60 mg	8 mL	7 mL	0.075
5	60 mg	8 mL	3 mL	0.082
6	60 mg	8 mL	0 mL	0.095

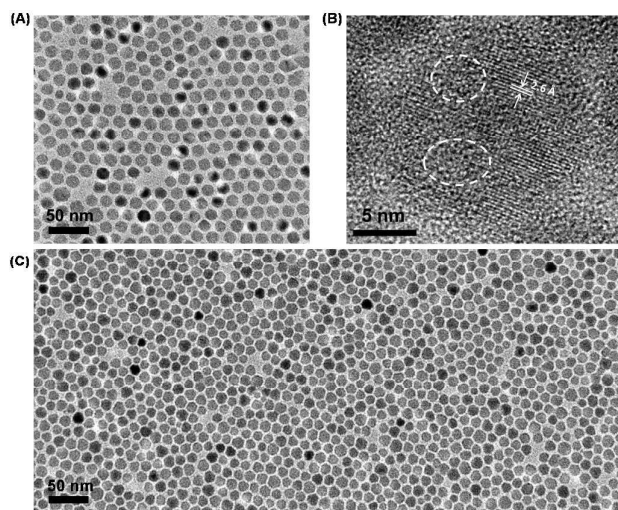


Fig. 1 (A) TEM image of the as-synthesized $\text{Ba}_{0.04}\text{-Fe-O}$ NPs. (B) HR-TEM image of a representative $\text{Ba}_{0.04}\text{-Fe-O}$ NP. (C) TEM image of the as-synthesized $\text{Ba}_{0.082}\text{-Fe-O}$ NPs.

Fig. 1A shows a typical transmission electron microscopy (TEM) image of the 15 ± 0.5 nm $\text{Ba}_{0.04}\text{-Fe-O}$ NPs. The high-resolution TEM image of a representative NP is shown in **Fig. 1B**. The distance of the lattice fringe was measured to be ~ 2.6

\AA , corresponding to the lattice spacing of (311) planes in the spinel Fe_3O_4 . Crystal defects are also visible in the NP as marked by the dashed circular lines, which can be ascribed to the lattice mismatch caused by the Ba doping. **Fig. 1C** shows the TEM image of the monodisperse $\text{Ba}_{0.082}\text{-Fe-O}$ NPs of 13 ± 0.5 nm. TEM images of the as-synthesized Ba-Fe-O NPs with other Ba compositions are shown in **Fig. S1†**. The Ba-Fe-O NPs were further characterized by energy dispersive X-ray (EDX) spectroscopy. **Fig. S2†** is the EDX spectrum of the $\text{Ba}_{0.082}\text{-Fe-O}$ NPs deposited on Si, confirming the existence of Ba and Fe at the atomic ratio of 0.093, which is close to that obtained from the ICP-AES analysis.

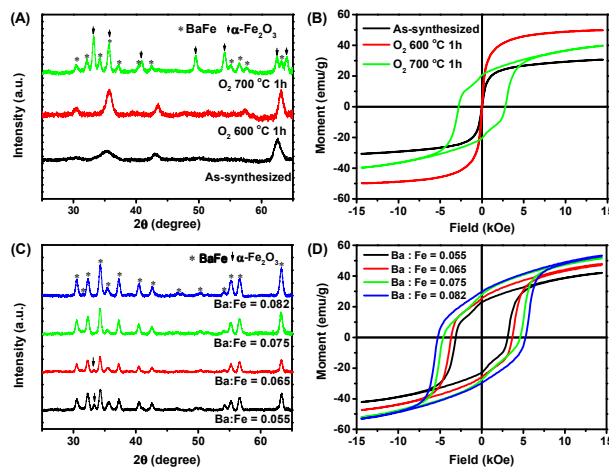


Fig. 2 (A) XRD patterns and (B) Room temperature hysteresis loops of the $\text{Ba}_{0.04}\text{-Fe-O}$ NPs before and after O_2 annealing treatment. (C) XRD patterns and (D) Room temperature hysteresis loops of the Ba-Fe-O NPs with different Ba compositions after annealing in O_2 at 700°C for 1 h.

X-ray diffraction (XRD) pattern of the as-synthesized $\text{Ba}_{0.04}\text{-Fe-O}$ NPs is shown in **Fig. 2A**. The pattern matches with the spinel Fe_3O_4 structure but the broad diffraction peaks infer the presence of small crystalline domains, which supports what is observed from **Fig. 1B**. The magnetic hysteresis loop of the as-synthesized $\text{Ba}_{0.04}\text{-Fe-O}$ NPs (**Fig. 2B**) indicates that these NPs are magnetically soft. Due to the existence of Ba and the induced crystal defects, the saturation moment (M_s) of the NPs is relatively small (31 emu/g) compared to the pure single crystalline Fe_3O_4 NPs at a similar size (~ 65 emu/g).³³ In order to convert the as-synthesized Ba-Fe-O NPs into BaFe NPs, we first tested different annealing conditions to ensure that Fe_3O_4 structure could be oxidized to $\alpha\text{-Fe}_2\text{O}_3$,³⁵ followed by the formation of BaFe phase via the diffusion of Ba^{2+} into $\alpha\text{-Fe}_2\text{O}_3$ lattice.³⁶ In O_2 at 600°C for 1 h, the $\text{Ba}_{0.04}\text{-Fe-O}$ NPs show no obvious structure change and diffraction peaks become sharper (**Fig. 2A**), indicating the annealing enlarges the crystal domain within each NP, which is further supported by their soft magnetic property with higher M_s than the as-synthesized NPs (**Fig. 2B**). $\text{Ba}_{0.082}\text{-Fe-O}$ NPs behave similarly once annealed the same way (**Fig. S3†**). When annealed at 700°C in O_2 for 1 h, the as-synthesized $\text{Ba}_{0.04}\text{-Fe-O}$ NPs are converted into hexagonal BaFe (**Fig. 2A**), which is ferromagnetic with the

coercivity (H_c) of 2800 Oe and M_s of 40 emu/g (Fig. 2B). Both XRD and magnetic data (the loop shows a two-phase behavior) indicate that in the annealed $Ba_{0.04}$ -Fe-O NPs, the α - Fe_2O_3 phase co-exists with the BaFe phase due to the non-stoichiometric composition of Ba in the NP structure. The increase of Ba composition from 0.055 to 0.065 reduces the amount of α - Fe_2O_3 presented in the annealed Ba-Fe-O NPs (Fig. 2C). When the Ba composition is above 0.075, no obvious diffraction peaks of α - Fe_2O_3 are observed for the annealed Ba-Fe-O NPs (Fig. 2C). The diffraction peaks of the annealed $Ba_{0.082}$ -Fe-O NPs match well with those of the hexagonal BaFe, indicating the formation of pure BaFe phase (Fig. 2C). It is worth noting that our annealing is performed at lower temperature and shorter time than previous syntheses,²⁴⁻²⁹ therefore, the NP morphology is better preserved.

Ba/Fe composition dependent magnetic properties of the annealed Ba-Fe-O NPs were studied and their hysteresis loops are shown in Fig. 2D. As the Ba composition increases from 0.055 to 0.082, the H_c of the annealed NPs increases from 3120 Oe to 5260 Oe (Fig. S4†). Their M_s increase as well from 42 emu/g to 54 emu/g due to the increased BaFe phase purity, which is further confirmed by the single-phase hysteresis loop from the annealed $Ba_{0.082}$ -Fe-O NPs. When the atomic ratio of Ba/Fe is over the optimal value required for the formation of BaFe (0.083) at 0.095, the annealed NPs show a decreased H_c (5150 Oe) and M_s (50 emu/g).

The above results demonstrate that the new synthetic method described in this paper is a facile approach to Ba-Fe-O and further to hard magnetic BaFe NPs. It is worth emphasizing that this synthetic method can be readily extended to the synthesis of Sr-Fe-O NPs. For example, by just replacing Ba(stearate)₂ with the same amount of Sr(stearate)₂ in the synthesis of $Ba_{0.082}$ -Fe-O NPs, Sr-Fe-O NPs were synthesized (Fig. S5†) with the size of 15 ± 1 nm. EDX spectrum of the as-synthesized NPs (Fig. S6†) confirms the Sr doping and the Sr/Fe ratio of 0.078. After annealed at 700 °C for 1 h in O₂, the NPs are ferromagnetic with the H_c of 4500 Oe and M_s of 50 emu/g (Fig. S7†), indicating the formation of hexagonal SrFe.

The as-synthesized Ba-Fe-O NPs are well dispersed in hexane, allowing easy self-assembly of these NPs into well-defined NP arrays. Using water-air interface self-assembly method,^{13,37} we fabricated a monolayer assembly of the $Ba_{0.082}$ -Fe-O NPs. Fig. 3A shows a TEM image of the monolayer assembly transferred onto a carbon coated Cu grid. SEM image of the monolayer array transferred onto a Si substrate is shown in Fig. 3B. After O₂ annealing at 700 °C for 1 h, the morphology of the monolayer was well maintained, as shown in Fig. 3C. No obvious NP sintering/aggregation in the monolayer array was observed. However, the magnetic signal generated from this monolayer array is too weak to be easily detected. To increase the magnetic signal from the assembly, we prepared a multilayer array of the $Ba_{0.082}$ -Fe-O NPs by drop-casting the NP dispersion (hexane, 0.5 mg/mL) directly on a Si substrate and by controlling the evaporation of hexane. Fig. 3D & S8† show the SEM images of the densely packed assemblies of the $Ba_{0.082}$ -Fe-O NPs. Different from the monolayer assembly that maintains the morphology after O₂ annealing

treatment, the multilayer assembly exhibits some NP aggregation/sintering after the same treatment (Fig. 3E). However, the grain size of the NPs after annealing is still around 50 nm. Room temperature magnetic properties of the annealed multilayer assembly were measured with the magnetic field perpendicular (out-of-plane) and parallel (in-plane) to the assembly plane. Fig. 3F is the hysteresis loops of the annealed assembly. The in-plane loop shows the H_c of 4100 Oe, which is much larger than that of the out-of-plane one ($H_c = 2050$ Oe). Moreover, the in-plane loop is squarer compared to the out-of-plane loop, suggesting the easy axis of the magnetization lies in the plane of the film. Such assembly may be especially useful to fabricate 3D stacks of BaFe NPs as new nanostructured magnets for energy product optimization.

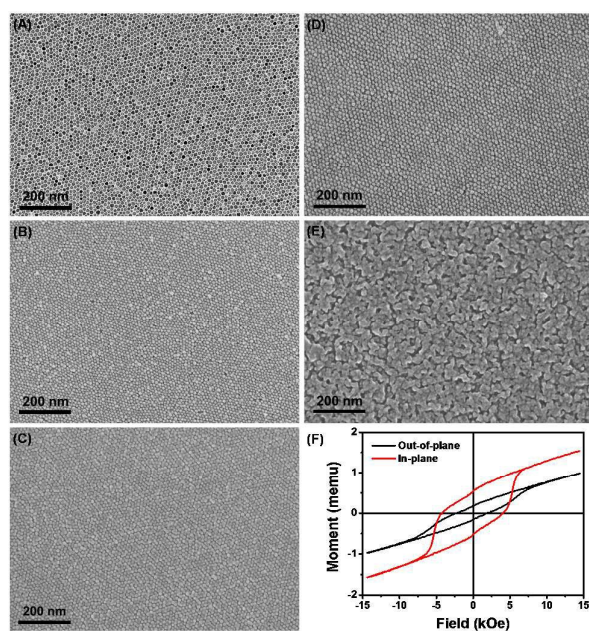


Fig. 3 (A) TEM image of the monolayer assembly of $Ba_{0.082}$ -Fe-O NPs. (B) SEM image of the monolayer assembly deposited on a Si substrate. (C) SEM image of the monolayer assembly after annealing in O₂ at 700 °C for 1 h. (D) SEM images of the multilayer assembly of $Ba_{0.082}$ -Fe-O NPs deposited on a Si substrate from the drop-casting method. (E) SEM image of the multilayer assembly after annealing in O₂ at 700 °C for 1 h. (F) Room temperature hysteresis loops of the multilayer assembly after annealing in O₂ at 700 °C for 1 h.

Conclusions

In conclusion, we have reported a facile organic-phase synthesis of monodisperse Ba-Fe-O NPs through thermal decomposition of Ba(stearate)₂ and Fe(acac)₃ in 1-octadecene with oleic acid and oleylamine as surfactants. The Ba/Fe composition is tuned from 0.04 to 0.095 by controlling the ratio of Ba(stearate)₂/Fe(acac)₃ or by the volume of oleylamine and 1-octadecene. The as-synthesized Ba-Fe-O NPs, especially the $Ba_{0.082}$ -Fe-O NPs, can be easily converted into

hexagonal BaFe by annealing in O₂ atmosphere at 700 °C for 1 h, showing strong ferromagnetic properties with H_c reaching 5260 Oe and M_s of 54 emu/g. More importantly, these monodisperse Ba-Fe-O NPs are well dispersed in hexane and can be easily assembled into densely packed 2D arrays and further converted into oriented BaFe magnets. Our reported synthetic method and self-assembly approach can also be extended to Sr-Fe-O and ferromagnetic SrFe NPs, providing a unique way of fabricating ferromagnetic ferrite arrays that may be important for magnetic energy storage and data storage applications.

Acknowledgements

This work was sponsored by the Critical Materials Institute, an Energy Innovation Hub funded by the U.S. Department of Energy, Office of Energy Efficiency and Renewable Energy, Advanced Manufacturing Office.

Notes and references

- J. T. Jang, H. Nah, J. H. Lee, S. H. Moon, M. G. Kim and J. Cheon, *Angew. Chem. Int. Ed.*, 2009, **48**, 1234.
- W. K. Moon, J. Kim, H. S. Kim, N. Lee, T. Kim, H. Kim, T. Yu, I. C. Song and T. Hyeon, *Angew. Chem. Int. Ed.*, 2008, **47**, 8438.
- K. Cheng, S. Peng, C. J. Xu and S. H. Sun, *J. Am. Chem. Soc.*, 2009, **131**, 10637.
- T. Hyeon, J. E. Lee, N. Lee, H. Kim, J. Kim, S. H. Choi, J. H. Kim, T. Kim, I. C. Song, S. P. Park and W. K. Moon, *J. Am. Chem. Soc.*, 2010, **132**, 552.
- J. H. Lee, Y. M. Huh, Y. Jun, J. Seo, J. Jang, H. T. Song, S. Kim, E. J. Cho, H. G. Yoon, J. S. Suh and J. Cheon, *Nat. Med.*, 2007, **13**, 95.
- J. H. Lee, J. T. Jang, J. S. Choi, S. H. Moon, S. H. Noh, J. W. Kim, J. G. Kim, I. S. Kim, K. I. Park and J. Cheon, *Nat. Nanotechnol.*, 2011, **6**, 418.
- C. Xu, J. Xie, D. Ho, C. Wang, N. Kohler, E. G. Walsh, J. R. Morgan, Y. E. Chin and S. Sun, *Angew. Chem. Int. Ed.*, 2008, **47**, 173.
- C. J. Xu, B. D. Wang and S. H. Sun, *J. Am. Chem. Soc.*, 2009, **131**, 4216.
- N. Poudyal and J. P. Liu, *J. Phys. D: Appl. Phys.*, 2013, **46**.
- J. Park, Y. K. Hong, S. G. Kim, S. Kim, L. S. I. Liyanage, J. Lee, W. Lee, G. S. Abo, K. H. Hur and S. Y. An, *J. Magn. Magn. Mater.*, 2014, **355**, 1.
- R. C. Pullar, *Prog. Mater. Sci.*, 2012, **57**, 1191.
- Q. Dai, D. Berman, K. Virwani, J. Frommer, P. O. Jubert, M. Lam, T. Topuria, W. Imaino and A. Nelson, *Nano Lett.*, 2010, **10**, 3216.
- L. Wu, P. O. Jubert, D. Berman, W. Imaino, A. Nelson, H. Zhu, S. Zhang and S. Sun, *Nano Lett.*, 2014, **14**, 3395.
- Z. V. Golubenko, L. P. Ol'khovik, Y. A. Popkov, Z. I. Sizova and A. S. Kamzin, *Phys. Solid State*, 1998, **40**, 1718.
- J. Wang, F. Zhao, W. Wu and G. M. Zhao, *J. Appl. Phys.*, 2011, **110**, 096107.
- D. Berman, R. Biskeborn, N. Bui, E. Childers, R. D. Cideciyan, W. Dyer, E. Eleftheriou, D. Hellman, R. Hutchins, W. Imaino, G. Jaquette, J. Jelitto, P. O. Jubert, C. Lo, G. McClelland, S. Narayan, S. Oelcer, T. Topuria, T. Harasawa, A. Hashimoto, T. Nagata, H. Ohtsu and S. Saito, *IEEE Trans. Magn.*, 2007, **43**, 3502.
- T. Harasawa, R. Suzuki, O. Shimizu, S. Olcer and E. Eleftheriou, *IEEE Trans. Magn.*, 2010, **46**, 1894.
- P. O. Jubert, R. Biskeborn, D. N. Qiu, A. Matsumoto, H. Noguchi and O. Shimizu, *IEEE Trans. Magn.*, 2011, **47**, 386.
- G. Cherubini, R. D. Cideciyan, L. Dellmann, E. Eleftheriou, W. Haeberle, J. Jelitto, V. Kartik, M. A. Lantz, S. Olcer, A. Pantazi, H. E. Rothuizen, D. Berman, W. Imaino, P. O. Jubert, G. McClelland, P. V. Koeppel, K. Tsuruta, T. Harasawa, Y. Murata, A. Musha, H. Noguchi, H. Ohtsu, O. Shimizu and R. Suzuki, *IEEE Trans. Magn.*, 2011, **47**, 137.
- S. Furrer, M. A. Lantz, J. B. C. Engelen, A. Pantazi, H. E. Rothuizen, R. D. Cideciyan, G. Cherubini, W. Haeberle, J. Jelitto, E. Eleftheriou, M. Oyanagi, Y. Kurihashi, T. Ishioroshi, T. Kaneko, H. Suzuki, T. Harasawa, O. Shimizu, H. Ohtsu and H. Noguchi, *IEEE Trans. Magn.*, 2015, **51**, 3100207.
- W. Zhong, W. P. Ding, Y. M. Jiang, N. Zhang, J. R. Zhang, Y. W. Du and Q. J. Yan, *J. Am. Ceram. Soc.*, 1997, **80**, 3258.
- L. Affleck, M. D. Aguas, Q. A. Pankhurst, I. P. Parkin and W. A. Steer, *Adv. Mater.*, 2000, **12**, 1359.
- J. Jin, S. Ohkoshi and K. Hashimoto, *Adv. Mater.*, 2004, **16**, 48.
- L. C. Li, K. Y. Chen, H. Liu, G. X. Tong, H. S. Qian and B. Hao, *J. Alloy Compd.*, 2013, **557**, 11.
- A. Yourdkhani, D. Caruntu, A. K. Perez and G. Caruntu, *J. Phys. Chem. C*, 2014, **118**, 1774.
- P. Xu, X. J. Han and M. J. Wang, *J. Phys. Chem. C*, 2007, **111**, 5866.
- J. Zhang, J. Fu, F. Li, E. Xie, D. Xue, N. J. Mellors and Y. Peng, *ACS Nano*, 2012, **6**, 2273.
- M. Manikandan and C. Venkateswaran, *J. Magn. Magn. Mater.*, 2014, **358**, 82.
- D. Lisjak and S. Ovtar, *J. Phys. Chem. B*, 2013, **117**, 1644.
- D. Primc and D. Makovec, *Nanoscale*, 2015, **7**, 2688.
- D. Primc, D. Makovec, D. Lisjak and M. Drofenik, *Nanotechnology*, 2009, **20**, 315605.
- J. Jalli, Y. K. Hong, S. Bae, G. S. Abo, J. J. Lee, J. C. Sur, S. H. Gee, S. G. Kim, S. C. Erwin and A. Moitra, *IEEE Trans. Magn.*, 2009, **45**, 3590.
- Z. C. Xu, C. M. Shen, Y. L. Hou, H. J. Gao and S. S. Sun, *Chem. Mater.*, 2009, **21**, 1778.
- S. Mourdikoudis and L. M. Liz-Marzan, *Chem. Mater.*, 2013, **25**, 1465.
- Y. L. Hou, Z. C. Xu and S. H. Sun, *Angew. Chem. Int. Ed.*, 2007, **46**, 6329.
- H. P. Steier, J. Requena and J. S. Moya, *J. Mater. Res.*, 1999, **14**, 3647.
- L. Wu, Q. Li, C. H. Wu, H. Zhu, A. Mendoza-Garcia, B. Shen, J. Guo and S. Sun, *J. Am. Chem. Soc.*, 2015, **137**, 7071.